EXPERIMENTAL AND NUMERICAL INVESTIGATION ON SHEAR RESPONSE OF STAINLESS STEEL PLATED GIRDERS

E Real
Universitat Politècnica de Catalunya

I Estrada
Universitat Politècnica de Catalunya

E Mirambell
Universitat Politècnica de Catalunya

Abstract

Resistance to shear is one of the most important load cases to be considered when designing slender steel plated structures. This is a widely studied issue in carbon steel but not in stainless steel structures due to its recent introduction into construction as structural material.

Given the conservative character of Eurocode 3, Part 1.4, it seems logical to apply other methods used in Eurocode 3 for carbon steel in order to determine more accurately the shear buckling resistance and the ultimate shear capacity in stainless steel plate structures taking into account the contribution of flanges. The tension field method and the rotated stress field method could be applied to stainless steel by adapting their design expressions to the new material properties.

This investigation has been divided into two experimental programmes. Data Generated in the first programme enabled the non-linear behaviour of stainless steel to be observed and some useful conclusions for designing stainless steel structures to be drawn.

On the other hand, the second experimental programme has been focussed on the response of stainless steel plated girders, mainly loaded in shear, attempting to identify the differences between the behaviour of the slender webs in girders with rigid and non-rigid end posts. Moreover, a comparative analysis of different design methods to determine shear resistance has been performed.

1 INTRODUCTION

The shear behaviour and the ultimate shear resistance of carbon steel plate girders have been studied extensively, resulting in the development of well established design methods, but not for stainless steel. The general approach for determining the shear resistance of webs in *ENV 1993-1-4 Design of steel structures: General rules-Supplementary rules for stainless steels* [1] is based on the simple post-critical method of *ENV 1993-1-1 Design of steel structures: General rules and rules for buildings* [2] that is simpler to apply than other methods proposed for carbon steel, but it results in a clearly conservative design.

Although both carbon and stainless steel design basis are very similar, these two materials present clearly different mechanical properties; material non-linearity of the stainless steel is the main difference between the two types of steel.

A numerical model in the FE-code ABAQUS [3] was used throughout the project.

After analysing the theoretical models, a numerical study allows us to understand the phenomenon, and enables the analyses of the behaviour of stainless steel plated girders subjected to shear and calibrating against tests. This previous analysis of the phenomenon becomes absolutely useful in terms of optimising the measurements taken during the test, because the important aspects of behaviour are known. Moreover, once validated with the experimental results, the numerical model becomes a powerful tool to analyse the phenomenon in detail.

1.1 Shear resistance in plated girders

When a plate is loaded in shear, equal tensile and compressive stress develop until that compression destabilizes the web making it buckle. The elastic critical shear buckling stress in a rectangular plate is given in the following equation, where the buckling factor for shear buckling k_s depends on the aspect ratio and boundary conditions.

$$\tau_{cr,i} = k_s \frac{\pi^2 E}{12(1-\nu^2)} \left(\frac{t_w}{d} \right)^2$$

It is widely known that web plates may exhibit a considerable post-critical strength reserve, first observed by Wilson [4] and afterwards explained by many other authors [5] [6] [7], that should be considered when designing steel plate girders. After buckling, the plate cannot carry further compressive stresses and a new load carrying mechanism develops, whereby any additional shear loading is supported by an inclined tensile stress field. As the applied loading increases, the tensile membrane stress grows until it reaches the yield stress of the material. When the web has yielded, final collapse will occur when plastic hinges are formed in the flanges that permit a shear sway failure mechanism.

Different theories have been developed to analyse the ultimate shear capacity of plate girders, and some of them are used in current design codes. These theories have been recently reviewed by Maquoi and Skaloud [8].

1.2 Design methods for steel plate girders

Design methods provided in Eurocode 3 are based on the Höglund's rotated stress field theory [9] and the tension field theory developed by Rockey et al [10].

ENV 1993-1-1 [2] includes two methods to calculate the shear capacity in plate girders, the simple postcritical method and the tension field method. The first one was developed on the basis of Höglund's model [11]. This model is characterised by assuming that after buckling, a stress redistribution starts, the web panel has no compression capacity and therefore the loads are carried by an increase in the principal tensile stress. This causes a rotation in principal stresses, and the web panel behaviour to be governed by a tension field. The ultimate shear strength is then reached when the yield criterion is fulfilled. Experience shows this method gives conservative results due to the fact that the flange's contribution to resisting shear is not considered in its formulation.

The second method proposed in ENV 1993-1-1 is based on the tension field. This theory supposes that once buckling occurs, the principal compressive stress is not able to increase, however the stresses in the perpendicular direction can still rise with the formation of a tension band which anchors in flanges and stiffeners. This tension field is developed until the moment that plastic hinges in flanges and stiffeners are formed. At this moment, a frame mechanism will cause the structure to collapse. Based on a statistical evaluation of the available experimental test results, this model was found to be especially adequate for aspect ratios smaller than 3 [8].

On the other hand, in *ENV 1993-1-5 Design of steel structures: General Rules-Supplementary rules for planar plated structures without transverse loading* [12] the rotated stress field method is proposed. This method is also based on Höglund's theory but in this case the design expressions include the flange contribution in the resistant mechanism that permits the development of a tension field anchored in them that make the shear capacity to increase. Now that Eurocodes are undergoing their last reviews before the final report, it seems the tendency is to remove both methods in ENV 1993-1-1 [2] and to maintain only the rotated stress field method.

1.3 Shear resistance in stainless steel plated girders

This field has been widely studied in carbon steel but only limited studies have been carried out in stainless steel plates. In stainless steel structures, shear buckling is always developed during the non-linear path and its postcritical behaviour is clearly influenced by the material non-linearity, which results in a loss of resistant capacity.

The first experimental work known to address the shear resistance of stainless steel members was carried out by Carvalho, Van den Berg and Van der Merwe [13]. These have been the only available tests studying shear resistance for long time, so the design curve adopted in ENV 1993-1-4 [1] is based on the simple postcritical method of ENV 1993-1-1 [2] taking into account the non-linear behaviour of the stainless steel.

The derived design curve was taken as the one which gave a satisfactory lower bound to the experimental data.

Recent studies in stainless steel shear buckling have been conducted in the Universitat Politècnica de Catalunya by Real [14] and in the University of Luleå by Olsson [15] where several experimental projects have been performed. Carrying out a comparative analysis, the results obtained by the application of the simple postcritical method proposed in ENV 1993-1-4 [1] have demonstrated this method to be extremely conservative.

2 NON-LINEAR BEHAVIOUR OF STAINLESS STEEL PLATED GIRDERS UNDER SHEAR LOADS

2.1 Experimental test

In order to analyse the non-linear behaviour of stainless steel plated girders under shear loads, an experimental programme was conducted. Tests were performed on nine girders covering a wide range of web slenderness values and several aspect ratios of the web panel, these being two determining factors of the element response under shear load.

The geometry of the tested girders was directly related to the objective of the experimental programme. Therefore, in order to minimise the flexural effects as compared to the shear ones, the beams were designed as short span and large depth members which were tested as simply supported beams subjected to a concentrated load at mid-span.

In order to study the behaviour of the tested beams under shear and to compare experimental, numerical and analytical results, it is necessary to know the material properties of the tested beams. The steel producer determined the material properties on the specimens extracted from every type of welded plate used (thickness 4, 6, 8 and 20 mm) according to ASTM [16]. The steel grade used for all plates was the austenitic grade 1.4301 (AISI 304). A summary of the beams dimensions and material properties is presented in Table 1.

Table 1 Beams dimensions and material properties.

Beam	L (mm)	a (mm)	d (mm)	t_w (mm)	t_f (mm)	t_s (mm)	σ_{yw} (N/mm^2)	E_w (N/mm^2)	σ_{yf} (N/mm^2)	E_f (N/mm^2)
ad1w8	1000	500	500	8	20	20	323.29	190940	266.75	187340
ad1w6	1000	500	500	6	20	20	323.38	177100	266.75	187340
ad1w4	1000	500	500	4	20	20	301.44	197240	266.75	187340
ad15w8	1500	750	500	8	20	20	323.29	190940	266.75	187340
ad15w6	1500	750	500	6	20	20	323.38	177100	266.75	187340
ad15w4	1500	750	500	4	20	20	301.44	197240	266.75	187340
ad2w8	2000	1000	500	8	20	20	323.29	190940	266.75	187340
ad2w6	2000	1000	500	6	20	20	323.38	177100	266.75	187340
ad2w4	2000	1000	500	4	20	20	301.44	197240	266.75	187340

The instrumentation scheme was selected after a preliminary stress analysis of the beams with a numerical simulation. From this study, two different responses in front of shear load were expected. Every one of the instrumentation schemes shown in Figure 1 corresponds to one of both response modes.

A group of strain gauges was located on the centre of the web plate in order to evaluate stress levels during the pure shear stress state. The strain gauges in the web were located to register the intensity and magnitude of the tension field when it developed. In the second instrumentation scheme, the strain gauges placed at the corner enabled the progress of strain to be measured in the zone where the tension field would anchor.

In addition, three displacement transducers were located at the mid-height of the plate to register the deformed shape of the web during shear buckling. Finally, to evaluate deflections, two displacement transducers were placed. The first one was located at the mid-span cross-section and the other one at the bearing section to measure possible bearing displacements.

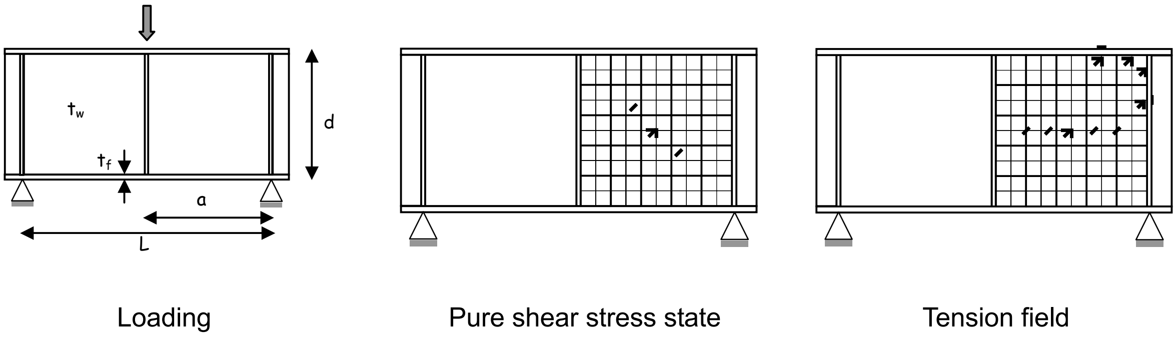

Figure 1 Loading and instrumentation schemes.

2.2 Experimental and numerical results

Experimental results obtained from the strain gauges and the displacement transducers were analysed and compared with the numerical ones. All the experimental results from this project can be found in [14] and [17].

In order to analyse the response of every beam, the experimental and numerical load-deflection curves were studied. In these curves, it is possible to identify the main changes in the behaviour of the beam. Moreover, this experimental curve is compared with that obtained by the numerical model (see Figure 2). The load-deflection curve in Figure 2 corresponds to a tested beam that has reached the shear buckling load level, where indicated.

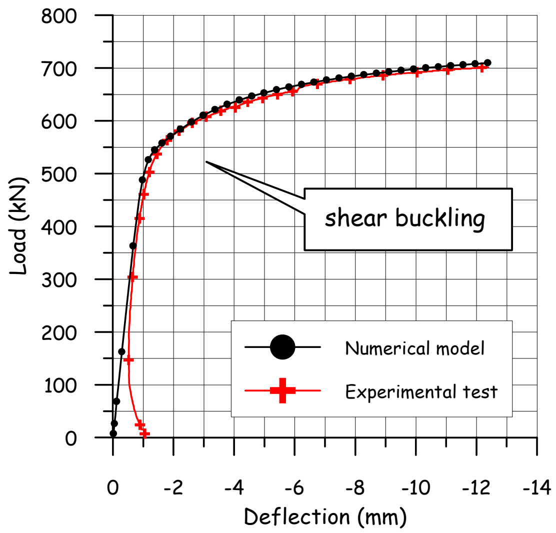

Figure 2 Load-deflection curve in ad1w4 beam test.

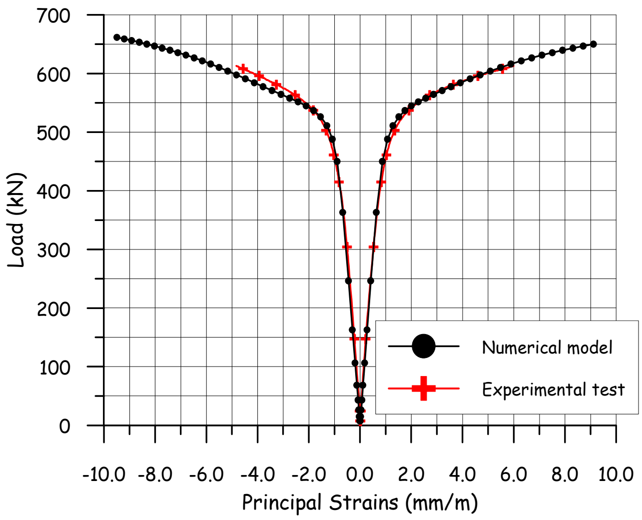

Figure 3 Load-principal strain curves in ad1w4 beam test.

Once the general behaviour of the girder is determined by the load-deflection curve, it is necessary to know the stress state of the beams during the tests. The results from the strain gauges are in strain terms. Moreover, the phenomenon study requires a stress analysis in order to improve the evaluation of the structural response of the beam. The structural element is subjected to a biaxial stress state in the presence of a non-linear material. Due to these facts, transforming the strains measured during the tests into stresses is not possible in a direct way by the constitutive equation. Therefore, the numerical model is used to compare both the experimental and numerical results in strains terms (Figure 3). Once the numerical model has been validated, it can be used to study the phenomenon in stress terms.

Using this procedure, a detailed analysis of the tested beams was conducted, and three different responses were detected. Figure 4 represents, in terms of deflection and stress evolution in the middle point of the panel, these different structural responses.

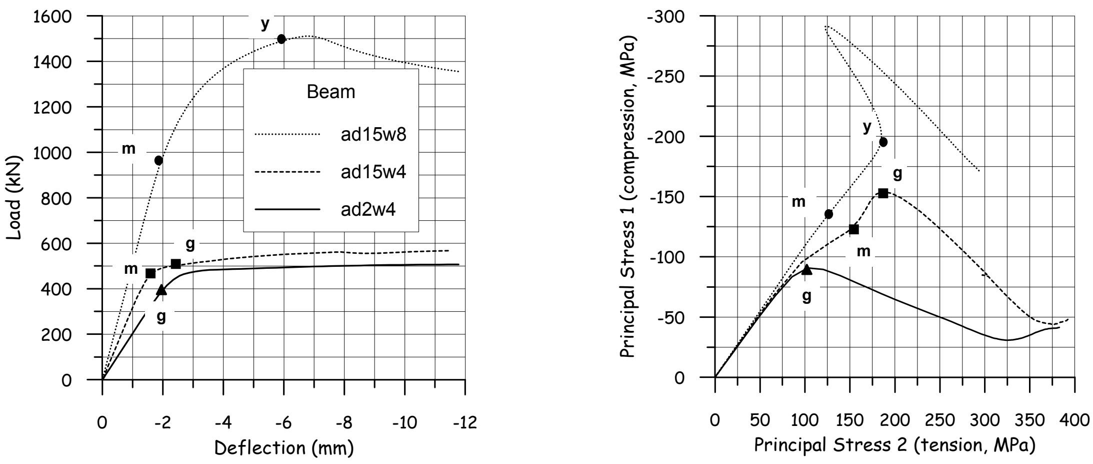

g:geometric non-linearity, m:material non-linearity, y:yielding

Figure 4 Structural responses observed in the tested beams with the numerical analysis.

In the most slender beam (ad2w4), buckling occurred in the elastic range. The material non-linearity appeared during the development of the tension field in the postcritical range. The change in the behaviour in the load-deflection curve is induced by the shear buckling of the web. This fact is confirmed by the analysis of the principal stresses. At the beginning of the test, principal stresses are equal and opposite, so the web panel is under a pure shear stress state. Once buckling occurs (point g), the web has no compression capacity and therefore, there is an increment of the principal tensile stress.

Beams ad1w4, ad15w4 and ad2w6 displayed a change in the load-deflection curve when material non-linearity appeared (point m). At that moment, the centre of the web was still under a pure shear stress state as it can be deduced from the fact that compressive and tensile principal stress values continued to increase at the same rate. After that, buckling occured as can be seen in the principal stresses graph when only tension can be developed (point g).

Finally, beams ad1w6, ad1w8, ad15w8 and ad2w8 were so stocky that yielding occurred before buckling occurred and were therefore subjected to pure shear stress state throughout the test. The loss of linearity in the load-deflection curve is due to the material non-linearity (point m) and during the loading procedure compressive and tensile stresses have the same value (opposite directions) until the moment that yielding occurs.

2.3 Critical shear buckling stress

The application of a new design method based on the tension field model like ENV 1993-1-1 [2] involves defining the initial shear buckling stress. Therefore the initial shear buckling stress defined in ENV 1993-1-4 [1] has been analysed.

A numerical model in the FE-code ABAQUS has been used to study the behaviour of simply supported stainless steel plates under shear loads. The results derived from the numerical model have been compared with those derived from ENV 1993-1-4 [1], and other analytical expressions obtained by the use of different plasticity reduction factors.

The American code ANSI/ASCE-8-90 [18] uses Gerard's plasticity reduction factor $\eta = G_s/G_0$. An experimental work conducted by Carvalho, van den Berg and van der Merwe [19], concluded that Gerard's plasticity reduction factor compares well with the experimental results.

Figure 5 shows the initial shear buckling stress for the plates analysed with the numerical model, the initial shear buckling stress proposed in Eurocode 3, Part 1-4 [1], and the elastic critical shear stress. Figure 5 also includes the curves obtained by using different plasticity reduction factors. The values of the initial shear buckling stress/yield shear stress are represented in the vertical axis. In this figure, it can be appreciated that $\eta = (G_t/G_0)^{1/2}$ is the plasticity reduction factor that approximates better with the results obtained from plates. It seems that the initial shear buckling stress proposed in Eurocode 3, Part 1-4 derives from the use of the $\eta = G_t/G_0$ plasticity reduction factor.

The shear stress-strain curved is derived from the normal stress-strain curve by using the affinity factors defined in [19], so:

$$\gamma = \frac{\tau}{G_0} + 0.002\beta\left(\frac{\tau}{\tau_y}\right)^n$$

with

$$G_0 = \frac{E_0}{2(1+\nu)} \quad \text{and} \quad \beta = 1.3$$

and

$$G_s = \frac{G_0}{1 + 0.002\beta G_0\left(\frac{\tau^{n-1}}{\tau_y^n}\right)} \quad \text{and} \quad G_t = \frac{\tau_y G_0}{\tau_y + 0.002\beta n G_0\left(\frac{\tau}{\tau_y}\right)^{n-1}}$$

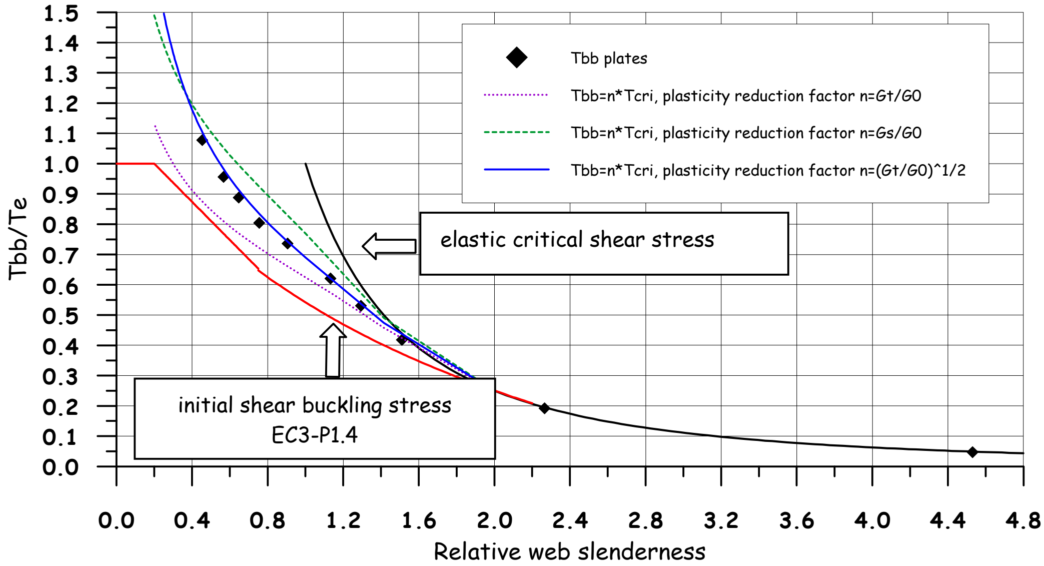

Figure 5 Initial shear buckling stress. Plasticity reduction factors.

It is important to point out that since G_s and G_t varies with stress and the buckling stress is a function of G_s or G_t, the approach requires iterations to find the shear buckling stress.

So, it is possible to define a unique expression of the initial shear buckling stress by approximating the curve obtained with the $\eta = (G_t/G_0)^{1/2}$ plasticity reduction factor for a S220 stainless steel. Then the initial shear buckling stress should be obtained from the table presented in Figure 6.

Figure 6 shows the initial shear buckling stress proposed in ENV 1993-1-4 [1], the elastic critical shear buckling stress, the initial shear buckling stress for the analysed plates with the numerical model and the curve obtained by using $\eta = (G_t/G_0)^{1/2}$ plasticity reduction factor. This figure also shows the initial shear buckling stress proposed. The values of the initial shear buckling stress/yield shear stress are represented in the vertical axis.

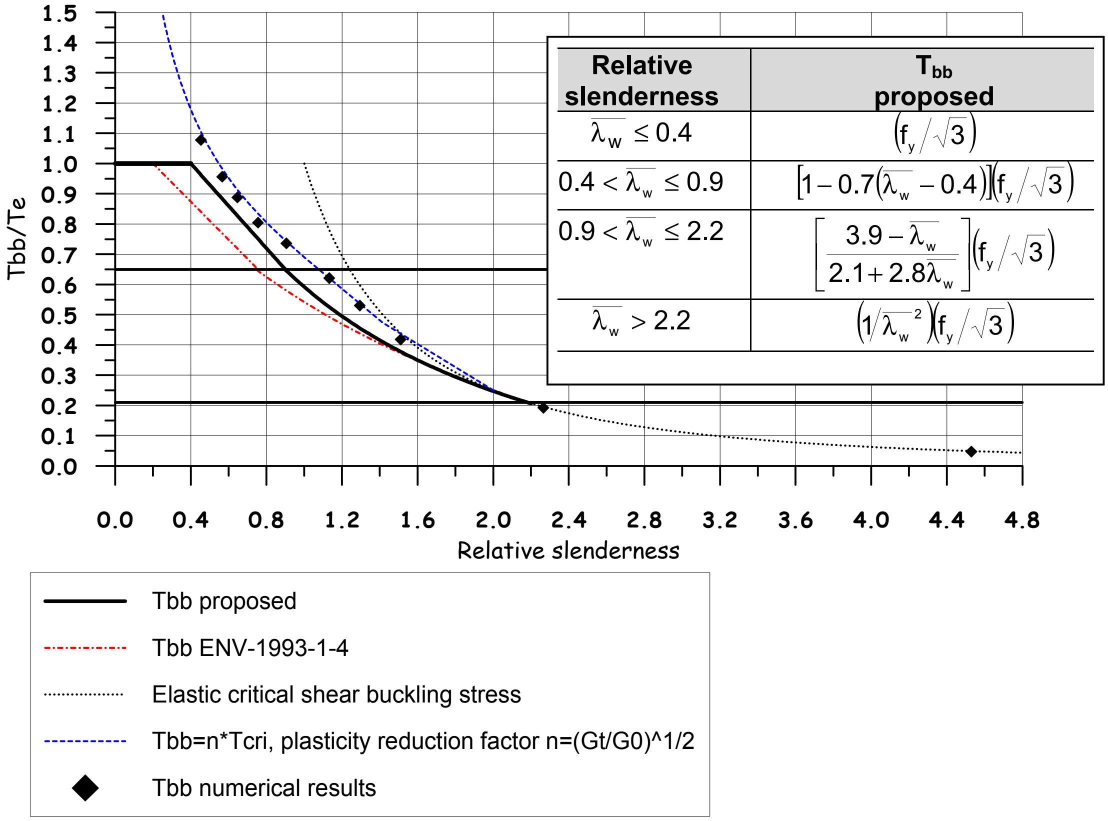

Relative slenderness	**T_{bb} proposed**
$\bar{\lambda}_w \leq 0.4$	$\left(f_y/\sqrt{3}\right)$
$0.4 < \bar{\lambda}_w \leq 0.9$	$\left[1-0.7\left(\bar{\lambda}_w-0.4\right)\right]\left(f_y/\sqrt{3}\right)$
$0.9 < \bar{\lambda}_w \leq 2.2$	$\left[\dfrac{3.9-\bar{\lambda}_w}{2.1+2.8\bar{\lambda}_w}\right]\left(f_y/\sqrt{3}\right)$
$\bar{\lambda}_w > 2.2$	$\left(1/\bar{\lambda}_w^{\,2}\right)\left(f_y/\sqrt{3}\right)$

Figure 6 Initial shear buckling stress.

2.4 Design methods

Following the analysis of the tested beams behaviour, the experimental results obtained for the ultimate shear load have been compared with those resulting from the numerical model and the ones calculated according to European design codes.

As explained earlier, ENV 1993-1-4 [1] proposes the simple postcritical method to determine the ultimate shear capacity in the same way as in ENV 1993-1-1 [2] for carbon steel, but adapting the expressions to stainless steel.

Table 2 shows the ultimate shear values obtained by the application of the simple postcritical method to stainless steel, alongside the numerical and the test results. On the other hand, ultimate shear loads are determined by the application of the tension field method proposed in ENV 1993-1-1[2] for carbon steel and adapting it to stainless steel. This adaptation to stainless steel consists in using the same design expressions to carbon steel but considering the mechanical properties and critical shear buckling load of stainless steel presented before.

Finally, an adaptation of the rotated stress method from ENV 1993-1-5 [13] for carbon steel to stainless steel is also analysed. This adaptation, first proposed in [15], is the design method included in [20].

Table 2 Ultimate shear load values (kN).

Beam	λw	V_{pl}	ENV 1993-1-4 Simple post-critical method	ENV 1993-1-1 Stainless Tension field method	ENV 1993-1-5 Stainless Rotated stress field method	Numerical model	Tests
ad2w4	1.553	348.1	165.6	240.4	207.5	255.3	242.9
ad15w4	1.465	348.1	171.4	273.1	228.6	293.0	284.4
ad1w4	1.279	348.1	185.3	324.3	275.3	363.6	352.5
ad2w6	1.131	560.1	318.6	426.4	395.9	466.6	-
ad15w6	1.068	560.1	328	467.2	429.5	483.5	-
ad1w6	0.932	560.1	350.1	533.4	505.9	530.9	-
ad2w8	0.817	746.6	494.6	652.5	648.8	713.5	-
ad15w8	0.771	746.6	506.7	693.3	695.7	755.7	-
ad1w8	0.673	746.6	534.3	755.8	804.6	803.6	-

Figure 7 shows a graphic representation of these results to give a better comparison. It is important to outline that the results are expressed in a non-dimensional form by using the plastic shear resistance value (V_{pl}).

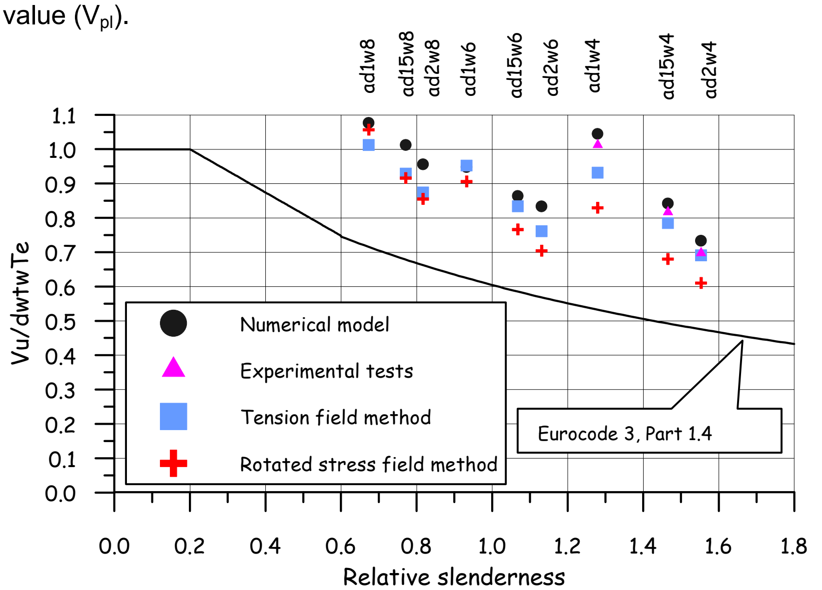

Figure 7 Graphic representation of shear capacity of tested beams.

Through comparison of the results, it is possible to observe that the numerical model provides a good approximation to the actual behaviour of the tested beams. Therefore, the numerical model can be used to compare the test results to those from analytical expressions. Notice that only for the three beams of 4 mm web thickness, it was possible to reach the ultimate shear load during the test due to the maximum load capacity of the testing machine.

An important conclusion reached during this work was the importance of the elements where the tension field anchors. Once the plate buckles, it can only resist an increment of load by increasing tension, and so a tension field band anchored in flanges and stiffeners is developed while rotating until the moment that the stiffness of these anchorage elements permits. In the tested beams it was observed that the final slope of this tension band coincided with the geometrical diagonal of the panel. This is a smaller capacity of rotation than that predicted in the theoretical models used in ENV 1993-1-1 [2] when considering full strength of the anchor elements, and results in a lower ultimate capacity.

From this point, a future direction to work appeared as a natural link to this first project. The study of the differences in the behaviour between intermediate and end panels and the effect of having a geometry of rigid or non-rigid end post.

3 PLATED GIRDERS WITH RIGID AND NON-RIGID END POST

3.1 Experimental tests

The aim of this experimental programme was to study the response of stainless steel plated girders under service loads and up to failure, with particular emphasis on the difference between the behaviour of beams with rigid and non-rigid end posts. Ten plate girders were tested in the Laboratory of Structural Technology in Technical University of Catalunya (UPC).

Beam	L mm	a mm	d mm	t_w mm	t_f mm	λ_w
nr700ad15	2360	1050	700	4	20	2.085
r700ad15	2360	1050	700	4	20	2.085
nr600ad2	2660	1200	600	4	20	1.894
r600ad2	2660	1200	600	4	20	1.894
nr500ad25	2760	1250	500	4	20	1.625
r500ad25	2760	1250	500	4	20	1.625
nr400ad325	2860	1300	400	4	20	1.329
r400ad325	2860	1300	400	4	20	1.329
i500ad1	2200	500	500	4	20	1.279
i500ad15	2700	750	500	4	20	1.465

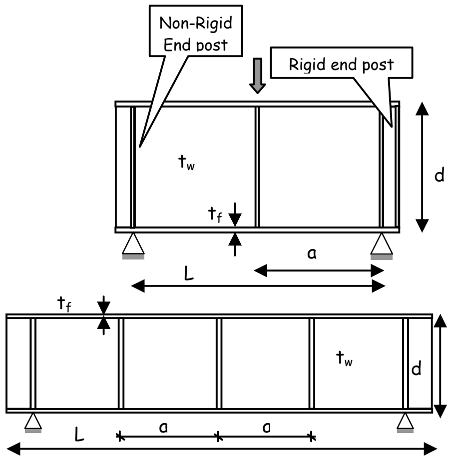

Figure 8 Geometry and load scheme of the tested beams.

The first eight beams consisted of four pairs of beams where each pair had the same geometrical and material characteristics with the only difference being that one had rigid end post (r-beams) while the other had non rigid end post (nr-beams). Moreover, two four-panel beams (see Figure 8) were tested with the geometry of the inner panels being the same as the panels of two beams tested in the first project described in section 2. The geometry, the main characteristics, and the general loading and support arrangement of the tested beams are presented in Figure 8.

The beam instrumentation in this experimental set-up consisted of uniaxial and triaxial strain gauges to measure deformations in web and flanges, and a set of linear displacement transducers to measure displacements.

The instrumentation scheme was selected after the preliminary stress analysis of the beams with the numerical simulation. After the results obtained in previous works [14], one of the most important points to analyse in this study was the evolution and the inclination in the tension band after the shear buckling. Therefore, three triaxial strain gauges were located in the central vertical axis of the web plate in order to evaluate stress levels during the pure shear stress state and to register the intensity, magnitude and mainly the slope of the tension field when it developed (see Figure 9). Moreover, the strain gauges placed at the corner of the web panel enabled the progression of the strain to be monitored in the zone where the tension field would be anchored. As to know how the anchorage elements of the tension band (flanges and stiffeners) progress in stresses, three uniaxial strain gauges were located in the points where the anchorage will take place.

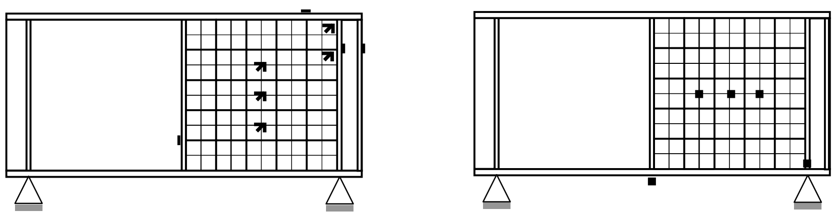

a. Strain gauges b. Displacement transducers

Figure 9 Instrumentation schemes.

In addition, the displacement transducers were located following the same scheme used in the previous project.

3.2 Experimental and numerical results

The analyses of the load-centre section deflection curve for every beam showed that the rigid end post results in increasing the ultimate capacity of the beam (see Figure 10).

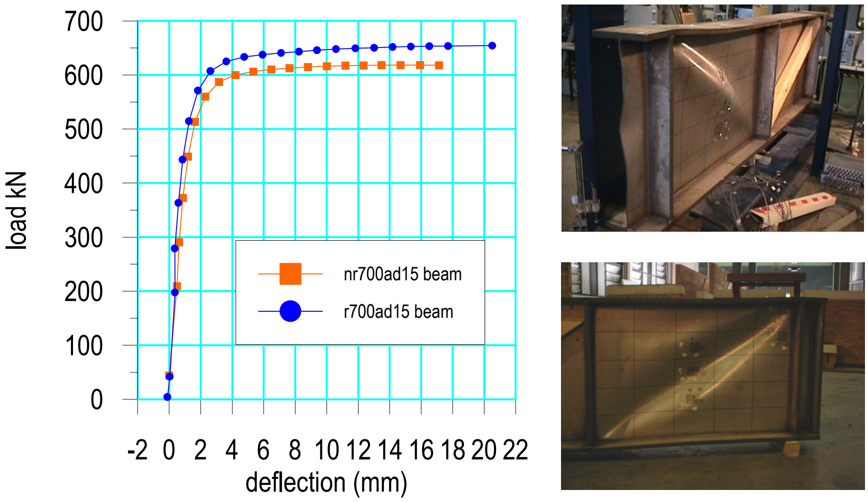

Figure 10 Comparison between rigid and non-rigid end post. nr700ad15 and r700ad15.

Once the behaviour of the beams had been studied, the ultimate shear load results obtained in the experimental project were compared with those resulting from the numerical model and the ones calculated from the methods in the ENV 1993-1-1 [2] and ENV 1993-1-5 [13], but with modification for stainless steel plate girders presented in [14] and [15] respectively. The results are presented in Table 5.

Table 5 Ultimate shear load values (kN).

Beam	λw	V_{pl}	ENV 1993-1-4 Simple post-critical method	ENV 1993-1-1 Stainless Tension field method	ENV 1993-1-5 Stainless Rotated stress field method	Numerical model	Tests
nr700ad15	2.085	969.9	379.86	504.15	454.70	628.76	618.42
r700ad15	2.085	969.9	379.86	587.50	454.70	686.03	654.34
nr600ad2	1.894	831.4	347.99	449.61	402.51	538.65	521.32
r600ad2	1.894	831.4	347.99	494.39	402.51	570.24	525.85
nr500ad25	1.625	692.8	320.38	421.34	365.62	463.26	456.03
r500ad25	1.625	692.8	320.38	439.22	365.62	462.28	473.09
nr400ad325	1.329	554.3	288.86	386.68	330.51	421.10	435.80
r400ad325	1.329	554.3	288.86	384.62	330.51	421.45	430.67

It is important to notice that in the design procedure proposed in [15], the difference between rigid and non-rigid end post is not taken into account.

Comparing results, it is possible to observe that numerical model provides a good approximation to the actual behaviour of the tested beams. Therefore, the numerical model can be used to compare the test results to those from analytical expressions.

On the other hand, the numerical and experimental results show that, when the end post of a plated girder is rigid, it provides an increase of the member capacity before shear develops.

4 DISCUSSION AND CONCLUSIONS

The experimental results obtained from the tests and further analysis of the experimental and numerical results, allow us to reach some conclusions related to the behaviour of stainless steel plate girders under shear loads.

From the comparative analysis of numerical and experimental results, it can also be concluded that the numerical model provides a good approximation to the actual behaviour of stainless steel structural elements. Thus it can be used as a useful analysis tool in order to develop and establish new design rules to incorporate into codes.

Also, the comparative analysis has enabled us to confirm that the behaviour of stainless steel plates under shear load is analogous to that of carbon steel plates. In the beams tested, a tension field band developed as a new resistant mechanism after reaching the shear buckling load level but this behaviour is clearly influenced by the material non-linearity.

From analysing experimental and numerical results, three different behaviours could be observed. In the most slender beams, shear buckling occurred before material non-linearity appeared. In beams with intermediate slenderness, the non linear material effect appeared before the geometric non-linearity. Finally, stocky beams were subjected to a pure shear stress state throughout the test.

On the other hand, it has been found that the simple postcritical method proposed in ENV 1993-1-4 [1] underestimates the ultimate resistance with respect to shear.

Therefore, new design methods to determine shear resistance in stainless steel beams should be evaluated in future studies. These methods are based on the adaptation to stainless steel of the tension field method proposed in ENV 1993-1-1 [2] and the rotated stress field method proposed in ENV 1993-1-5 [12] for carbon steel structures.

The application of a new design method based on the tension field model as in ENV 1993-1-1 [2] involves defining the initial shear buckling stress. Therefore the initial shear buckling stress defined in ENV 1993-1-4 [1] has been analysed and a new expression for the initial shear buckling stress for stainless steel plates has been proposed.

On the other hand, due to the fact that the rotated stress field method seems to be the only one included in the definitive Eurocodes, it becomes natural to adapt it to stainless steel taking into account the influence of the rigidity in the end post of the beam. Tests carried out in plate girders with rigid and non-rigid end post permit to observe that, when the end post of a plated girder is rigid, it provides an increase in member capacity.

Continuing with this research line and in order to evaluate all the design cases of plate girders that can be found in construction, a new experimental programme is being prepared to study the effects of introducing a longitudinal stiffener in the behaviour of stainless steel plate girders loaded mainly in shear.

This work aims to extend the study of shear behaviour in stainless steel beams and to establish new design expressions more adjusted to reality in order to introduce them into codes and enable stainless steel to be used cost-effectively and safely in structures.

5 ACKNOWLEDGMENTS

This research work was carried out under the financial support provided by the Spanish Ministries of Education and Culture and of Science and Technology as part of the Research Projects PB95-0772 and MAT 2000-1000 respectively. The second author was also supported from a grant awarded by the Universitat Politècnica de Catalunya since January 2001. We also appreciate the collaboration of Inoxcenter and URSSA for providing the material for tests.

6 REFERENCES

[1] European Committee for Standardisation, 1996. ENV 1993-1-4. Eurocode 3: Design of Steel Structures. Part 1.4:General rules- Supplementary Rules for Stainless Steel. Brussels.

[2] European Committee for Standardisation, 1993. ENV 1993-1-1. Eurocode 3: Design of Steel Structures. Part 1.1: General Rules and Rules for Buildings. Brussels.

[3] Hibbit, Karlsson and Sorensen Inc. ABAQUS/Standard, Version 5.6. Users Manual. Rhode Island, USA, 1996.

[4] Wilson, J.M., On Specifications for Strength of Iron Bridges, Transactions of the American Society of Civil Engineers, 15, Part I, 1886, 40-403, 489-490.

[5] Basler, K., Strength of Plate Girders in Shear, 1961. Journal of the Structural Division, Proc. ASCE, 87, (ST7). 151-180

[6] Rockey, K.C. and Skaloud, M., 1972 The Ultimate Load Behaviour of Plated Girders Loaded in Shear, Structural Engineer, 50, (1), 29-47

[7] Roca, P., Mirambell, E. and Costa, J., 1996, Geometric and Material Nonlinearities in Steel Plates, Journal o f Structural Engineering, ASCE, Vol.122, No.12, December

[8] Maquoi, R. and Skaloud, M., 2000, Stability of plates and plated structures. General Report. Journal of Constructional Steel Research 55 (2000) 45-68.

[9] Höglund, T., 1998. Shear buckling resistance of steel and aluminium plate girders, Thin-walled Structures, 29 (1-4). 13-30.

[10] Rockey, K.C., Evans, H.R. and Porter, D.M., 1978. A Design Method for Predicting the Collapse Behaviour of Plate Girders, Proceedings of the Institution of Civil Engineers, 65. 85-112.

[11] Davies, A.V. and Griffith, D.S.C., 1999. Shear strength of steel plate girders. Proc. Instn. Civ. Engrs. Structs & Bldgs. 134. 147-157

[12] European Committee for Standardisation, 1997, ENV 1993-1-5. Eurocode 3: Design of Steel Structures. Part 1.5:General rules- Supplementary rules for planar plated structures without transverse loading. Brussels.

[13] Carvalho, E.C.G., Van den Berg, G.J. and Van der Merwe, P., April 1990. Local Shear Buckling in Cold-Formed Stainless Steel Beam Webs. Proceedings of the Annual Technical Session, Structural Stability Research Council.

[14] Real, E. 2001. Aportaciones al estudio del comportamiento a flexión de estructuras de acero inoxidable. Doctoral Thesis. Dept. Ingeniería de la Construcción, Universitat Politécnica de Catalunya. Barcelona, Spain.

[15] Olsson, A., 2001. Stainless Steel Plasticity. Material modelling and structural applications. Doctoral thesis. Department of Civil and Mining Engineering. Lulea University of Technology. Lulea, Sweden

[16] American Society for Testing and Materials. Standard Practice for Numering Metals and Alloys (UNS), E527. Philadelphia, 1990.

[17] Real,E., Estrada, I. and Mirambell, E. 2001. Campaña experimental para el análisis del fenómeno de la abolladura por cortante en vigas armadas de acero inoxidable. Dept. Ingeniería de la Construcción. UPC-ETSECCP.

[18] ANSI/ASCE-8-90, 1991, American Society of Civil Engineers. Specification for the Design of Cold-formed Stainless Steel Structural Members. New York, NY.

[19] Carvalho, E.C.G., Van den Berg, G.J. and Van der Merwe, P., 1992. Behaviour of cold-formed stainless steel beams subjected to shear. In SSRC 1992 Annual Session, Earthquake Stability Problems in Eastern North America, pages 141-157. Structural Stability Research Council. Pittsburgh, Pennsylvania

[20] Euroinox, 2002. Design manual for structural stainless steel. Second Edition. The European Stainless Steel Development Association and the Steel Construction Institute, Oxford, UK.